The localization of VAMP5 in skeletal and cardiac muscle

Authors

Maiko Takahashi, Yuki Tajika, Astrid Feinisa Khairani, Hitoshi Ueno, Tohru Murakami, Hiroshi Yorifuji

Affiliations

Department of Anatomy, Gunma University Graduate School of Medicine

This is the pre-peer reviewed version of the following article: Maiko Takahashi, Yuki Tajika, Astrid Feinisa Khairani, Hitoshi Ueno, Tohru Murakami, Hiroshi Yorifuji. *The localization of VAMP5 in skeletal and cardiac muscle.* Histochem Cell Biol. 2013, which has been published in final form at http://link.springer.com/article/10.1007%2Fs00418-012-1050-0

Corresponding Author

Hiroshi Yorifuji, MD, PhD

Department of Anatomy, Gunma University Graduate School of Medicine, 3-39-22 Showa-machi, Maebashi, Gunma 371-8511, Japan,

TEL: +81-27-220-7912, FAX: +81-27-220-7916

E-mail: yorifuji@gunma-u.ac.jp

Proofs to: Maiko Takahashi, t-maiko@med.gunma-u.ac.jp

Abstract

VAMP5 (Vesicle-Associated membrane Protein 5) is a member of the SNARE protein family, which is generally thought to regulate the docking and fusion of vesicles with their target membranes. This study investigated the expression and localization of the VAMP5 protein. Immunoblotting analyses detected the VAMP5 protein in skeletal muscle, heart, spleen, lung, liver, and kidney tissue but not in brain or small intestine tissue. Through the immunofluorescence microscopy of skeletal muscle, we found that the expression level of VAMP5 varies among fibers. Most of the fibers with high expression levels of VAMP5 were categorized as type IIa fibers on the basis of their myosin heavy chain (MyHC) subtypes. In addition, the expression patterns of VAMP5 and glucose transporter 4 (GLUT4) were similar. In cardiac muscle, we determined that VAMP5 was localized to the vicinity of intercalated discs. These results suggest that VAMP5 plays local roles in membrane trafficking in skeletal and cardiac muscle.

Keywords

VAMP5, SNARE, skeletal muscle, cardiac muscle, vesicle trafficking,

membrane fusion

Introduction

Mammalian skeletal muscle is composed of highly specialized structures for contraction, and this tissue has characteristic development and regeneration features. During the course of muscle differentiation, myoblasts proliferate and fuse to form multinuclear myotubes, which subsequently mature into myofibers. Myofibers have unique membrane structures, such as the sarcolemma, the T-tubule, and the sarcoplasmic reticulum. If the sarcolemma is damaged by mechanical stress during contraction and extension, then membrane fusion processes occur to repair and regenerate the myofibers (Towler et al. 2004). These processes are thought to involve specialized membrane trafficking functions (Towler et al. 2004). Membrane trafficking is a fundamental event in various types of cells, but the details of the trafficking in myofibers are relatively unknown. To gain insight into membrane trafficking in myofibers, we investigated the presence of soluble N-ethylmaleimide-sensitive factor attachment protein receptor (SNARE) proteins in skeletal muscle (Tajika et al. 2008; Tajika et al. 2007; Tajika et al. 2010).

SNARE proteins are regarded as key components of the protein complexes that drive membrane fusion (Jahn and Scheller 2006). SNAREs are thought to ensure the specific distribution of

membrane proteins in the plasmalemma and various organelles (Chen and Scheller 2001). Vesicular SNAREs (v-SNAREs) interact with their target SNAREs (t-SNAREs) to form SNARE complexes that mediate membrane fusion (Chaineau et al. 2009). Seven v-SNARE isoforms have been identified, and these isoforms are called vesicle-associated membrane proteins (VAMPs). VAMP5 was found during a database search and subsequently cloned (Zeng et al. 1998). Northern blot analyses have indicated that the mRNA for VAMP5 is predominantly detected in heart and skeletal muscle (Zeng et al. 1998). Immunoblotting assays have detected the VAMP5 protein in mouse skeletal muscle and heart tissue but not in brain tissue (Schwenk et al. 2010). However, no analysis of the localization and function of VAMP5 *in vivo* has been performed.

In the present study, we performed immunofluorescence analyses to determine the expression and localization of VAMP5 in skeletal and cardiac muscle. We found that VAMP5 was expressed in the type IIa fibers of skeletal muscle and that in cardiomyocytes, VAMP5 expression was localized to the vicinity of intercalated discs.

Materials and Methods

Animals

C57BL/10ScN mice (4 to 5 months of age) were obtained from the Central Institute for Experimental Animals (Kawasaki, Japan). The mice were deeply anesthetized by the inhalation of diethyl ether and the intraperitoneal injection of pentobarbital and perfused with phosphate-buffered saline (PBS) to remove the blood from their organs. Various organs were quickly dissected out and used for immunoblotting and immunofluorescence microscopy. The protocol that was used in this study was approved by the Animal Care and Experimentation Committee of Gunma University (#10-061).

Cell culture

C2C12 myoblasts were obtained from the RIKEN Cell Bank (Tsukuba, Japan). To induce differentiation, $4x10^5$ cells in 3.5-cm dishes or $7x10^4$ cells/well in 24-well plates were grown in DMEM containing 10% fetal bovine serum for 24 hr and then incubated in DMEM containing 2% horse serum. The medium was replaced approximately every 24 hr prior to the use of the cells.

RNA interference

siRNAs (AAAUUGUUGAGCAUGAUUUCCGUCA and UUCUGCUGGGCUAAAGUCUUGGUUG) that targeted nucleotides 132–156 and 246–470 of the VAMP5 sequence (NM_016872) were

purchased from Invitrogen (Stealth RNA, Carlsbad, CA, USA). Mutated siRNAs (AAAGCUGUUUAGCGUAAGUUCUUCA and UUCGGUGUCGUCGGGAAAUUCUUUG) were used as controls. These siRNAs were designated as 1, 2, 1m, and 2m, respectively. Cells in 24-well plates were transfected with siRNAs by lipofection (Lipofectamine 2000, Invitrogen) in accordance with the manufacturer's recommended protocol. Cells from each well were homogenized and used for western blot analyses.

Immunoblotting

Samples of the tibialis anterior (TA) muscle, extensor digitorum longus (EDL) muscle, soleus (SOL) muscle, heart, brain, spleen, lung, liver, small intestine, and kidney were homogenized in sample buffer (0.25 M Tris-HCl (pH 6.8), 40% glycerol, 8% SDS, 5% 2-mercaptoethanol, and 20% bromophenol blue). The homogenates were denatured at 100°C for 5 minutes and stored at -30°C until use. The protein concentrations were determined using a Bio-Rad protein assay (Hercules, CA, USA). Proteins (50 μg/lane) were run on 13% polyacrylamide gels and transferred onto a PVDF membrane. After blocking with 3% bovine serum albumin (BSA) in rinse buffer (10 mM Tris-HCl (pH 7.5), 0.15 M NaCl, 1 mM EDTA, and 0.1% Triton X-100) for 2 to 3 hours, the membrane was incubated first with primary

antibodies and subsequently with HRP-labeled secondary antibodies. The following antibodies were used: rabbit anti-VAMP5 antibody (1:5,000; Synaptic Systems, Goettingen, Germany) (Rose et al. 2009; Schwenk et al. 2010), mouse anti-desmin antibody (1:500; clone DE-R-11; Leica Microsystems, Newcastle-upon-Tyne, UK), rabbit anti-glyceraldehyde-3-phosphate dehydrogenase (GAPDH) antibody (1:2,000; clone 14C10; Cell Signaling Technology, Danvers, MA), rabbit anti-actin antibody (1:2,000; Kanto Chemical Co, Inc, Tokyo, Japan), HRP-conjugated donkey F(ab')$_2$ fragments against rabbit IgG (1:50,000; Jackson ImmunoResearch, West Grove, PA, USA), and mouse IgG (1:50,000; Jackson ImmunoResearch). Chemiluminescence (ImmunoStar LD; Wako, Osaka, Japan) was detected using a cooled CCD camera (QICAM; Qimaging, Surrey, BC, Canada) with a 25-mm lens (F=0.95). The specificity of these assays was assessed by incubation with an anti-VAMP5 antibody in the presence of 0.01 μg/ml recombinant VAMP5 protein, which was used to raise the antibody (amino acids 1-70, 1:6000; Synaptic Systems), or by assays involving the omission of the primary antibody.

Immunofluorescence microscopy

Fresh muscular tissues were embedded in OCT compound (Sakura Finetek, Tokyo, Japan) and rapidly frozen in 2-methylbutane chilled with liquid nitrogen. The samples were then stored at −80°C until use. Transverse sections (which were each 7 μm thick) were cut with a Leica CM1900 cryostat (Vienna, Austria) and placed on poly-L-lysine-coated glass slides. The sections were washed with PBS and blocked with MOM blocking reagent (Vector Laboratories, Burlingame, CA) in PBS. The specimens were first incubated with primary antibodies and subsequently incubated with fluorescently labeled secondary antibodies. The following primary antibodies were used: rabbit anti-VAMP5 antibody (1:1,000; Synaptic Systems), mouse anti-spectrin antibody (1:200; clone NCL-SPEC2, Leica), mouse anti-type I myosin heavy chain (MyHC) antibody (1:500; clone NOQ7.5.4D, Sigma, St. Louis, MO, USA), mouse anti-type II MyHC antibody (1:100; clone MY-32, Sigma), mouse anti-type IIa MyHC antibody (1:50; clone A4.74, Developmental Studies Hybridoma Bank, Iowa City, IA, USA), mouse anti-embryonic MyHC antibody (1:20; clone F1.652, Developmental Studies Hybridoma Bank), mouse anti-glucose transporter 4 antibody (1:100; clone 1F8, Cell Signaling), mouse anti-N-cadherin antibody (1:500; clone 32/N-cadherin, BD transduction Laboratories Franklin Lakes, NJ USA), mouse anti-desmoplakin antibody (1:500; clone DP1&2-2.15,

DP1-2.17, DP1&2-2.20, Progen Biotechnik, Heidelberg Germany) and mouse anti-connexin 43 antibody (1:50; clone CX-1B1, Invitrogen). The following secondary antibodies were used: Rhodamine RedX- or Cy5-conjugated donkey antibodies against rabbit or mouse IgG (1:500; Jackson ImmunoResearch) and Alexa Fluor-488-conjugated phalloidin (1:50; Invitrogen). Nuclear DNA was stained with DAPI (1:200; 10 mg/ml saturated solution). As immunohistochemical controls, sections were reacted with anti-VAMP5 antibody in the presence of 0.01 μg/ml recombinant VAMP5 protein. The specimens were examined with an Olympus IX81 fluorescence microscope equipped with the FluoView FV1000 confocal system (Olympus, Tokyo, Japan). Images were processed using either FV10-ASW 1.6 (Olympus) or Adobe Photoshop CS4 (Adobe Systems, San Jose, CA, USA).

Image analysis

The TA and SOL muscles were obtained from 3 mice. Sections were immunostained for VAMP5 and spectrin. Spectrin is a member of the sarcolemmal membrane skeleton and was used to define the area of each muscle fiber. The images were initially obtained as 12-bit images without the saturation of signals and subsequently converted to 8-bit images. The mean intensity of

VAMP5 in a muscle fiber was calculated using the ImageJ plug-ins 'Image Calculator' and 'Analyze Particles' (http://rsb.info.nih.gov/ij/, National Institutes of Health, Bethesda, MD, USA). To categorize the muscle fibers into type I MyHC, type IIa MyHC, type IIb MyHC, and type IIx MyHC, serial sections were stained with MyHC isoform antibodies. The antibody against type IIa (clone A4.74) also recognizes type IIx to a lesser extent (Peters et al. 1997). Type IIb fibers were defined as type II (clone MY-32)-positive and type IIa (clone A4.74)-negative fibers.

Cardiotoxin injection

Cardiotoxin from *Naja mossambica mossambica* was purchased from Sigma (St. Louis, MO, USA) and diluted in sterile 0.9% NaCl. Animals (3 months of age) were anesthetized by the inhalation of diethyl ether. A single dose (50 μl) of cardiotoxin (10 μM) mixed with carbon ink, which was used as an indicator of successful administration, was injected into the TA muscles of two mice. The animals were processed for immunohistochemistry at 1 and 3 weeks after the injection.

Results

VAMP5 was expressed in various mouse organs but not the brain or the small intestine.

The characteristics of the polyclonal antibody against VAMP5 were assessed by immunoblotting. We confirmed that VAMP5 produced a band of ~15 kDa in C2C12 cells, and that the VAMP5 level increased during myogenesis *in vitro* (Fig. 1a, upper panel). These are consistent with previously published reports (Zeng et al. 1998, Schwenk et al. 2010). Desmin, a muscle-specific intermediate filament, and GAPDH were detected as a differentiation marker and a loading control, respectively (Fig. 1a, middle and bottom panels). RNAi was performed for the further characterization of the antibody (Fig. 1b). The transfection of C2C12 cells with a VAMP5-specific siRNA decreased the level of VAMP5 proteins (upper panel, lanes labeled as 1 and 2), whereas the transfection of C2C12 cells with a mutated siRNA did not affect the VAMP5 level (upper panel, lanes labeled as 1m and 2m). These results indicate that the antibody specifically recognizes VAMP5. Using this anti-VAMP5 antibody, we analyzed lysates of skeletal muscles (TA, EDL, and SOL) by immunoblotting and found that VAMP5 appeared as a single band (Fig. 1c, left panel). The disappearance of this band with the addition of recombinant VAMP5 protein (Fig. 1c, right panel) indicated that the antibody recognized VAMP5 specifically. In

addition, we determined the VAMP5 expression in various organs, and we found that the VAMP5 protein was also expressed in the heart, spleen, lungs, liver, and kidneys but not in the brain or the small intestine (Fig. 1d).

The expression level of VAMP5 varies among myofibers.

The localization of VAMP5 in skeletal muscle was determined by immunofluorescence microscopy in the TA and SOL muscles; the former is rich in fast-twitch fibers, whereas the latter is rich in slow-twitch fibers. Serial sections were immunostained with anti-VAMP5 antibody in the absence (Fig. 2a and b) or presence (Fig. 2e and f) of recombinant VAMP5 protein. We found that VAMP5 was expressed at different levels in each myofiber (Fig. 2a and b). Myofibers marked with circles and triangles in Fig. 2 provide examples of strong and weak VAMP5 signals, respectively. The addition of recombinant VAMP5 protein abolished the VAMP5 signals (Fig. 2e and f). Spectrin staining revealed the outline of each myofiber and allowed for the evaluation of the mean intensity of VAMP5 per cross sectional area of each fiber (Fig. 2c, d, g, and h). The mean intensities of VAMP5 are plotted in Figure 2i. The data points that are marked by circles and triangles represent the VAMP5 intensities of the marked myofibers in Figure 2a and b respectively,

indicating the VAMP5 intensity differences in each myofiber.

VAMP5 is expressed preferentially in type IIa muscle fibers.

Rodent skeletal muscle consists of four types of fibers that are distinguished by their myosin heavy chain (MyHC) subtypes; in particular, these fibers include slow-twitch fibers (type I) and fast-twitch fibers (type IIa, IIb, IIx/d). Serial sections of TA and SOL muscles were immunostained for VAMP5 (Fig. 3a and e) and MyHC (types I, II, and IIa) (Fig. 3b-d and f-h) to compare the VAMP5 levels between different fiber types. After the categorization of the fibers into the four fiber types, we found that VAMP5 is expressed preferentially in type IIa fibers (Fig. 3i). The graph of VAMP5 intensity also suggests that smaller fibers express higher levels of VAMP5 (Fig. 3i, left). To determine whether small myofibers are immature fibers, we examined the expression of VAMP5 during muscle regeneration (Fig. 4). Cardiotoxin injections were used to injure TA muscles to induce muscle regeneration, and the immunofluorescence of the injured muscles was assessed at 1 and 3 weeks after this injury. VAMP5 expression was weak at 1 week after a cardiotoxin injection but became strong by 3 weeks after an injection (Fig. 4a_1 and c_1). At 1 week after the injury, immature fibers were positive for embryonic MyHC, whereas these fibers were

negative for VAMP5 (Fig. 4, the arrowheads of the upper panel). At 3 weeks after injury, myofibers that had differentiated to a greater extent expressed adult-type MyHC instead of embryonic MyHC (Fig. 4, lower panel). VAMP5-positive fibers were primarily found in type IIa MyHC-positive fibers (Fig. 4c_1 and c_2); this observation was consistent with the results from mature skeletal muscle (Fig. 3). These findings indicate that VAMP5-positive type IIa fibers are small in size but are not immature.

The possible involvement of VAMP5 in the trafficking of transmembrane proteins.

We performed double-immunostaining for VAMP5 and glucose transporter 4 (GLUT4) to gain insight into the role of VAMP5. It has been reported that VAMP5, VAMP2, and VAMP7 coimmunoprecipitate with GLUT4 vesicles from skeletal muscle and move to the cell membrane simultaneously with GLUT4 translocation (Rose et al. 2009). This report suggests that these three VAMPs may be involved in the translocation of GLUT4. To verify that VAMP5 associates with GLUT4, we compared the localizations of VAMP5 and GLUT4. The expression levels of VAMP5 and GLUT4 varied among myofibers in a similar manner (Fig. 5a_1 and a_2). This result is consistent with our findings from the current study (Fig. 2 and 3) and

with previous reports that GLUT4 is enriched in type IIa and type I fibers rather than in type IIb fibers (Marette et al. 1992). Examining the subcellular localization of these two proteins, we found that VAMP5 partially colocalized with GLUT4 in the perinuclear and subsarcolemmal areas (as indicated by the arrows in Fig. 5b). In certain cytoplasmic regions, VAMP5 and GLUT4 were independently distributed (as indicated by the arrowheads in Fig. 5b). These results suggest that VAMP5 was partially associated with GLUT4 in skeletal muscle.

In cardiac muscle, VAMP5 was localized to the vicinity of intercalated discs.

Because VAMP5 protein was also detected in cardiac muscle by immunoblotting (Fig. 1d), the localization of VAMP5 was analyzed by immunofluorescence microscopy. VAMP5 was located strongly around the end of the cardiomyocytes (closed arrowheads in Fig. $6a_1$ and $6c_1$) and the perinuclear regions (open arrowheads in Fig. $6a_1$ and $6c_1$). VAMP5 was also found weakly throughout the cytoplasm of cardiomyocytes between myofibrils (arrows in Fig. 6c). At the long ends of cardiomyocyte, there are intercalated discs connecting adjacent cardiomyocytes. We performed double-immunostaining for VAMP5 and markers for three types of

junctions at the intercalated disc; adherence junction (N-cadherin, Fig. 6e_2), desmosome (desmoplakin, Fig. 6f_2) and gap junction (connexin 43, Fig. 6g_2). VAMP5 was found closely to these markers, indicating that VAMP5 was preferentially localized to the vicinity of intercalated discs (Fig. 6e_3, f_3 and g_3).

Discussion

In this study, we determined the expression and localization of VAMP5 in skeletal and cardiac muscle by immunoblotting and immunofluorescence microscopy. In skeletal muscle, the expression level of the VAMP5 protein varies among myofibers (Fig. 2), and VAMP5 is preferentially expressed in type IIa fibers but not in immature fibers (Fig. 3 and 4). The VAMP5 localization was primarily subsarcolemmal and cytoplasmic in myofibers (Fig. 5). In cardiac muscle, VAMP5 was preferentially localized to the vicinity of intercalated discs and to the perinuclear region (Fig. 6). In addition to its presence in muscle, VAMP5 was expressed in the spleen, lungs, liver, and kidneys but not in the brain (Fig. 1d), suggesting that VAMP5 is primarily involved in a trafficking pathway in non-neuronal tissues.

Both the lungs and the small intestine contain smooth muscle;

however, VAMP5 is present in lungs but is absent in the small intestine (Fig. 1d). This result suggests that smooth muscle does not express VAMP5. This differential expression may due to the difference in the cell types that are present in these two organs. Indeed, immunofluorescence assays of lung samples indicated that VAMP5 was present in bronchial epithelial cells but not in smooth muscle cells (data not shown).

Zeng Q and colleagues reported that as myoblasts were fused and differentiated into myotubes, their VAMP5 expression increased, suggesting that VAMP5 is associated with myogenesis (Zeng et al. 1998). However, in our *in vitro* experiments, C2C12 cells could differentiate into myotubes even if VAMP5 expression was suppressed (Fig. 1b). This result suggests that VAMP5 is not necessary for myogenesis. In addition, *in vivo* studies have revealed various VAMP5 expression levels in mature muscle fibers (Fig. 2). Type IIa fibers expressed VAMP5 at a higher level, whereas type IIb and I fibers expressed VAMP5 at lower levels (Fig. 3), indicating that distinct requirements for VAMP5 are found among different types of fibers. Thus, we suggest that VAMP5 may not play significant roles in myogenesis but may regulate intracellular trafficking events, which are fiber-type specific.

The VAMP5 localization was primarily subsarcolemmal and

cytoplasmic (perinuclear) in myofibers (Fig. 5). This localization pattern is consistent with the report that VAMP5 is localized to the plasma membrane and to intracellular vesicular structures in cultured C2C12 cells (Zeng et al. 1998). Given the VAMP5 localization in myofibers, what trafficking event is regulated by VAMP5? One possibility is GLUT4 translocation. GLUT4 is known to be translocated from the trans-Golgi network (TGN) to the cell surface upon insulin stimulation (Bryant et al. 2002; Shewan et al. 2003). In myofibers, GLUT4 is distributed in the perinuclear region, the sarcolemma and the T-tubules (Lauritzen et al. 2008; Ploug et al. 1998). In the current study, we found that the GLUT4 localization pattern overlapped with the localization pattern of VAMP5; in skeletal muscles, VAMP5 colocalized with GLUT4 in the perinuclear and subsarcolemmal regions of the examined samples but not in other areas (Fig. 5). Rose AJ and colleagues have demonstrated that upon insulin stimulation, VAMP5 coimmunoprecipitated with GLUT4 vesicles and was found at the cell surface (Rose et al. 2009). These data suggest that VAMP5 may be involved in certain pathways that are associated with GLUT4 translocation. In addition to VAMP5, VAMP2 and VAMP7 are also reported to be associated with GLUT4 (Rose et al. 2009). VAMP2 is expressed in the satellite cells of mature myofibers and in immature fibers (Tajika et al. 2007). VAMP2

partially colocalizes with GLUT4 in rat skeletal muscle (Tajika et al. 2007). VAMP7 has also been detected in skeletal muscle (Sato et al. 2011), but its precise subcellular localization has not been elucidated. The previously published reports and our findings from the current study suggest that not only VAMP5 but also other VAMPs may coordinate the intracellular trafficking of GLUT4.

In cardiac muscle, we found that VAMP5 was preferentially localized to the vicinity of intercalated discs and to perinuclear regions (Fig. 6). Intercalated discs consist of three major structures: adherens junctions, desmosomes, and gap junctions. These discs allow for intercellular communication by receiving mechanical tension at adherens junctions and desmosomes and then passing electrical stimuli and small molecules through channels at gap junctions (Noorman et al. 2009). The proteins that make up these junctions are transported from the perinuclear region to the intercalated discs by vesicular trafficking. Vesicle-like membrane structures have been visualized by electron microscopy (Berthoud 2004; Hoyt et al. 1989; Severs et al. 1989). Connexin 43 (Cx43), a component of gap junctions, is transported along microtubules after biogenesis, most likely by kinesin-based vesicular trafficking, and is then inserted into the plasma membrane (Smyth et al. 2010; Smyth et al. 2012). Cx43 is a short-lived protein with a half-life of several

hours (Beardslee et al. 1998). It is known that Cx43 turns over rapidly and that its regulation plays an important role in gap junction remodeling (Beardslee et al. 1998). These data raise the possibility that the transport and turnover of Cx43 might be highly regulated by SNARE proteins, including VAMP5, that are located near intercalated discs in cardiac muscle. Although we tried to determine the precise localization of VAMP5 protein at the intercalated disc using antibodies specific for each three junction, we could not specify it at the light microscopic level. Further studies are needed to elucidate the role of VAMP5 in both skeletal and cardiac muscle.

Acknowledgments

We thank H. Matsuda, M. Shikada and Y. Morimura for both technical and administrative assistance. This work was supported in part by Grants-in-Aid for Scientific Research from the Ministry of Education, Culture, Sports, Science, and Technology of Japan.

References

Beardslee MA, Laing JG, Beyer EC, Saffitz JE (1998) Rapid turnover of connexin43 in the adult rat heart. Circ Res 83:629–635.

Berthoud V (2004) Pathways for degradation of connexins and gap junctions. Cardiovascular Research 62:256–267. doi: 10.1016/j.cardiores.2003.12.021

Bryant NJ, Govers R, James DE (2002) REGULATED TRANSPORT OF THE GLUCOSE TRANSPORTER GLUT4. Nat Rev Mol Cell Biol 3:267–277. doi: 10.1038/nrm782

Chaineau M, Danglot L, Galli T (2009) Multiple roles of the vesicular-SNARE TI-VAMP in post-Golgi and endosomal trafficking. FEBS Letters 583:3817–3826. doi: 10.1016/j.febslet.2009.10.026

Chen YA, Scheller RH (2001) SNARE-mediated membrane fusion. Nat Rev Mol Cell Biol 2:98–106. doi: 10.1038/35052017

Hoyt RH, Cohen ML, Saffitz JE (1989) Distribution and three-dimensional structure of intercellular junctions in canine myocardium. Circ Res 64:563–574.

Jahn R, Scheller RH (2006) SNAREs — engines for membrane fusion. Nat Rev Mol Cell Biol 7:631–643. doi: 10.1038/nrm2002

Lauritzen HPMM, Galbo H, Brandauer J, et al. (2008) Large GLUT4 Vesicles Are Stationary While Locally and Reversibly Depleted During Transient Insulin Stimulation of Skeletal Muscle of Living Mice: Imaging Analysis of GLUT4-Enhanced Green Fluorescent Protein Vesicle Dynamics. Diabetes 57:315–324. doi: 10.2337/db06-1578

Marette A, Richardson JM, Ramlal T, et al. (1992) Abundance, localization, and insulin-induced translocation of glucose transporters in red and white muscle. Am J Physiol 263:C443–52.

Noorman M, van der Heyden MAG, van Veen TAB, et al. (2009) Cardiac cell-cell junctions in health and disease: Electrical versus

mechanical coupling. Journal of Molecular and Cellular Cardiology 47:23–31. doi: 10.1016/j.yjmcc.2009.03.016

Peters MF, Adams ME, Froehner SC (1997) Differential association of syntrophin pairs with the dystrophin complex. The Journal of Cell Biology 138:81–93. doi: 10.2307/1618124

Ploug T, van Deurs B, Ai H, et al. (1998) Analysis of GLUT4 distribution in whole skeletal muscle fibers: identification of distinct storage compartments that are recruited by insulin and muscle contractions. The Journal of Cell Biology 142:1429–1446.

Rose AJ, Jeppesen J, Kiens B, Richter EA (2009) Effects of contraction on localization of GLUT4 and v-SNARE isoforms in rat skeletal muscle. AJP: Regulatory, Integrative and Comparative Physiology 297:R1228–R1237. doi: 10.1152/ajpregu.00258.2009

Sato M, Yoshimura S, Hirai R, et al. (2011) The Role of VAMP7/TI-VAMP in Cell Polarity and Lysosomal Exocytosis in vivo. Traffic 12:1383–1393. doi: 10.1111/j.1600-0854.2011.01247.x

Schwenk RW, Dirkx E, Coumans WA, et al. (2010) Requirement for distinct vesicle-associated membrane proteins in insulin- and AMP-activated protein kinase (AMPK)-induced translocation of GLUT4 and CD36 in cultured cardiomyocytes. Diabetologia 53:2209–2219. doi: 10.1007/s00125-010-1832-7

Severs NJ, Shovel KS, Slade AM, et al. (1989) Fate of gap junctions in isolated adult mammalian cardiomyocytes. Circ Res 65:22–42.

Shewan AM, van Dam EM, Martin S, et al. (2003) GLUT4 Recycles via a trans-Golgi Network (TGN) Subdomain Enriched in

Syntaxins 6 and 16 But Not TGN38: Involvement of an Acidic Targeting Motif.

Smyth JW, Hong T-T, Gao D, et al. (2010) Limited forward trafficking of connexin 43 reduces cell-cell coupling in stressed human and mouse myocardium. J Clin Invest 120:266. doi: 10.1172/JCI39740

Smyth JW, Vogan JM, Buch PJ, et al. (2012) Actin cytoskeleton rest stops regulate anterograde traffic of connexin 43 vesicles to the plasma membrane. Circ Res 110:978–989. doi: 10.1161/CIRCRESAHA.111.257964

Tajika Y, Murakami T, Sato M, et al. (2008) VAMP2 is expressed in myogenic cells during rat development. Dev Dyn 237:1886–1892. doi: 10.1002/dvdy.21596

Tajika Y, Sato M, Murakami T, et al. (2007) VAMP2 is expressed in muscle satellite cells and up-regulated during muscle regeneration. Cell Tissue Res 328:573–581. doi: 10.1007/s00441-006-0376-0

Tajika Y, Takahashi M, Hino M, et al. (2010) VAMP2 marks quiescent satellite cells and myotubes, but not activated myoblasts. Acta Histochem Cytochem 43:107–114. doi: 10.1267/ahc.10010

Towler MC, Kaufman SJ, Brodsky FM (2004) Membrane Traffic in Skeletal Muscle. Traffic 5:129–139. doi: 10.1111/j.1600-0854.2003.00164.x

Zeng Q, Subramaniam V, Wong S, et al. (1998) A novel synaptobrevin/VAMP homologous protein (VAMP5) is increased during in vitro myogenesis and present in the plasma membrane. Mol Biol Cell 9:2423–2437.

Figures

Fig. 1 The immunoblot analyses of the VAMP5 protein. a: The level of VAMP5, which is represented by the band at 15 kDa, increased during the differentiation of C2C12 cells. The middle and bottom panels indicate bands for desmin and GAPDH, which were used as a differentiation marker and as a loading control, respectively. b: siRNAs were transfected into C2C12 cells on days 3 and 6 of differentiation, and the homogenate that was prepared on day 8 was analyzed. VAMP5-specific siRNAs (the lanes that are labeled 1 and 2) reduced the levels of VAMP5 protein, whereas mutated siRNAs (the lanes that are labeled 1m and 2m) did not affect the VAMP5 levels. As a control, cells were treated with liposomes alone (con). The expression levels of desmin and GAPDH were unaffected by the siRNA treatment (middle and bottom panels). c: VAMP5 was detected in skeletal muscle (TA, EDL, and SOL, 50 μg/lane). These bands disappeared after incubation with an anti-VAMP5 antibody in the presence of excess recombinant VAMP5 protein. d: VAMP5 was also detected in the heart, spleen, lungs, liver and kidneys but not in the brain or the small intestine (50 μg/lane).

Figure1

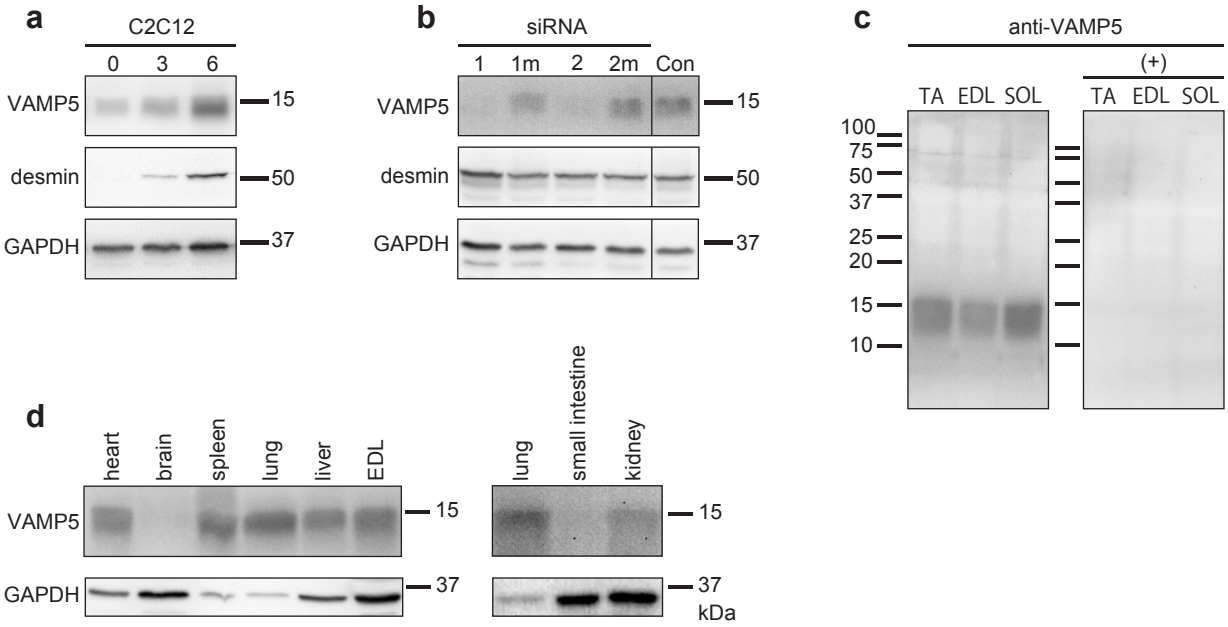
a
C2C12
0
3
6
VAMP5
15
desmin
50
GAPDH
37
b
siRNA
1
1m
2
2m
Con
VAMP5
15
desmin
50
GAPDH
37
c
anti-VAMP5
(+)
TA
EDL
SOL
TA
EDL
SOL
100
75
50
37
25
20
15
10
d
heart
brain
spleen
lung
liver
EDL
lung
small intestine
kidney
VAMP5
15
15
GAPDH
37
37
kDa

Fig. 2 The localization of VAMP5 in TA and SOL muscles. a-h: Transverse sections of TA and SOL muscles were labeled for VAMP5 (a, b). Simultaneously, sections were labeled for spectrin, a component of the sarcolemmal membrane skeleton, to define the margin of each muscle fiber (c, d). To confirm the specificity of the antibody, serial sections were incubated with anti-VAMP5 and anti-spectrin antibodies in the presence of recombinant VAMP5 protein (e-h). The addition of recombinant protein abolished the signals for VAMP5 (e, f). The left and right panels correspond to TA and SOL, respectively. Bar = 50 μm. i: The mean intensity of the VAMP5 signal per fiber was calculated for the TA muscle (132 fibers) and the SOL muscle (188 fibers). The intensities of the VAMP5 signals in the absence and the presence of the recombinant protein are plotted in black and gray, respectively. The data points that are indicated with circles and triangles correspond to the fibers that are shown in a-d. The bars represent the mean values ± SD.

Figure2

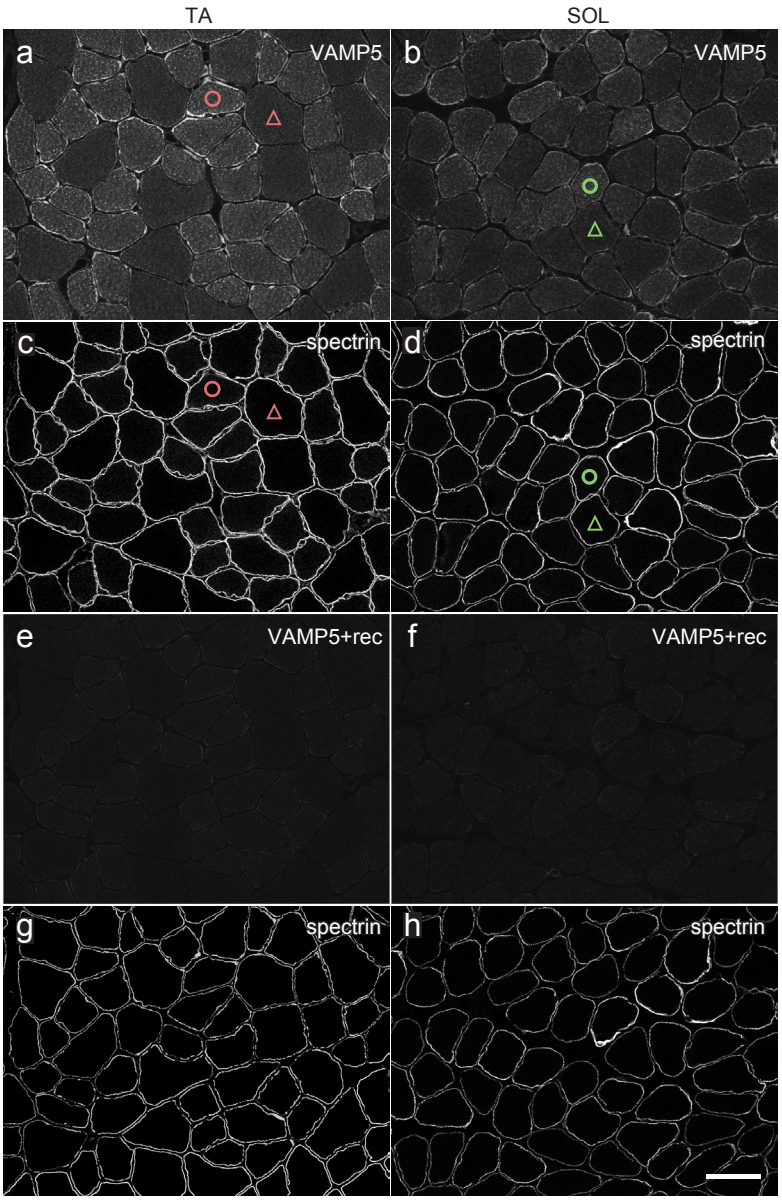
TA
SOL
a
VAMP5
b
VAMP5
c
spectrin
d
spectrin
e
VAMP5+rec
f
VAMP5+rec
g
spectrin
h
spectrin

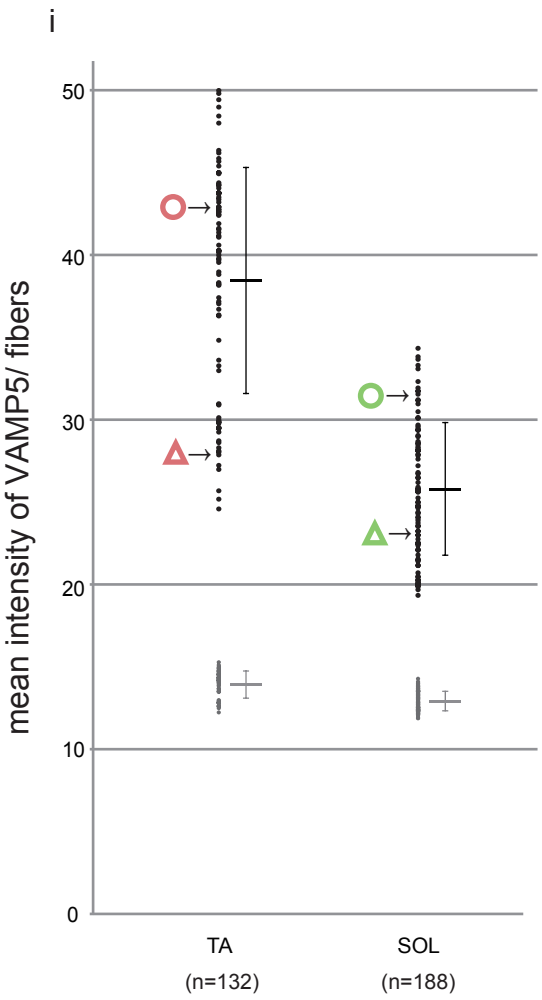
i
mean intensity of VAMP5/ fibers
50
40
30
20
10
0
TA
(n=132)
SOL
(n=188)

Fig. 3 VAMP5 is preferentially expressed in type IIa muscle fibers. To categorize the muscle fiber types, four serial sections were labeled for VAMP5 and spectrin (a, e), type IIa myosin heavy chain (MyHC; b, f), type II MyHC (c, g), and type I MyHC (d, h). Fluorescence images for each MyHC were projected onto the corresponding Nomarski images (b-d, f-h). The antibody against type IIa MyHC (clone: A4.74) also recognizes type IIx to a lesser extent. Type IIb fibers were defined as fibers stained with type II MyHC but not with type IIa MyHC. Bar = 50 μm. Scatter plots of the VAMP5 intensity and cross-section are provided (i, left: TA, right: SOL). The red, blue, gray, and yellow data points represent type IIa, IIb, IIx, and I muscle fibers, respectively.

Figure3

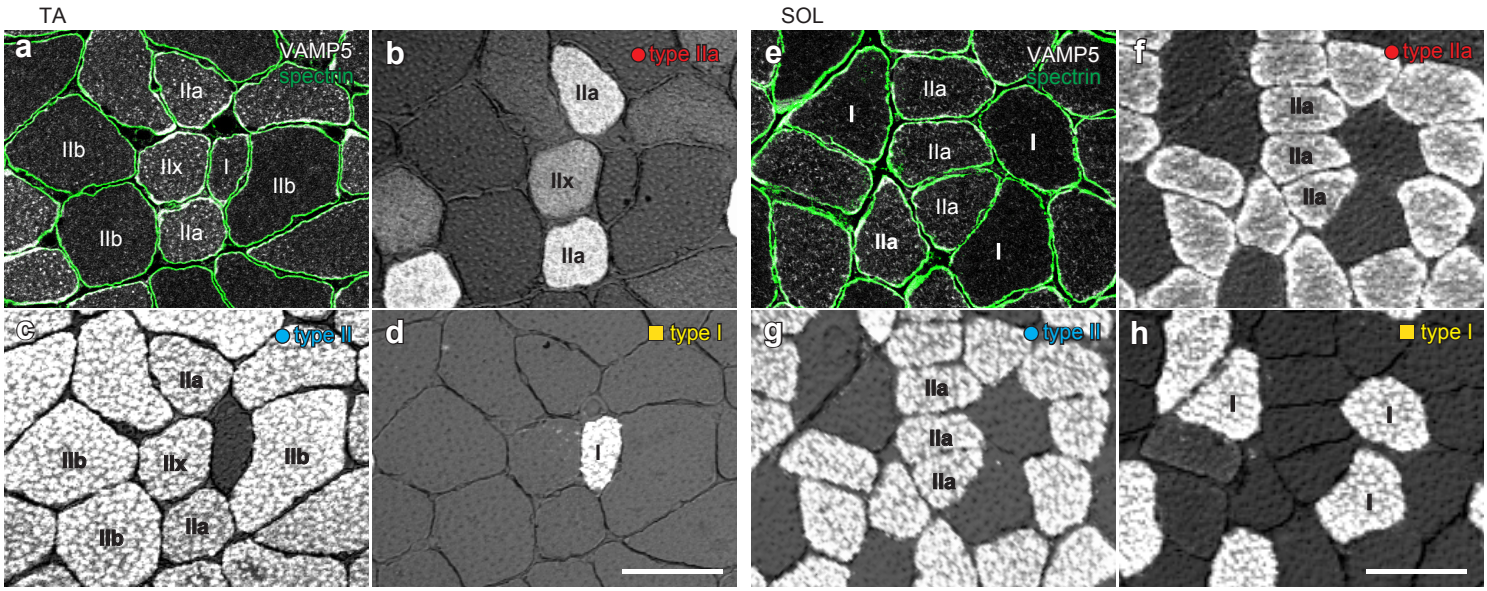
TA
SOL
a
VAMP5
spectrin
IIa
IIb
IIx
I
b
type IIa
c
type II
d
type I
e
f
g
h

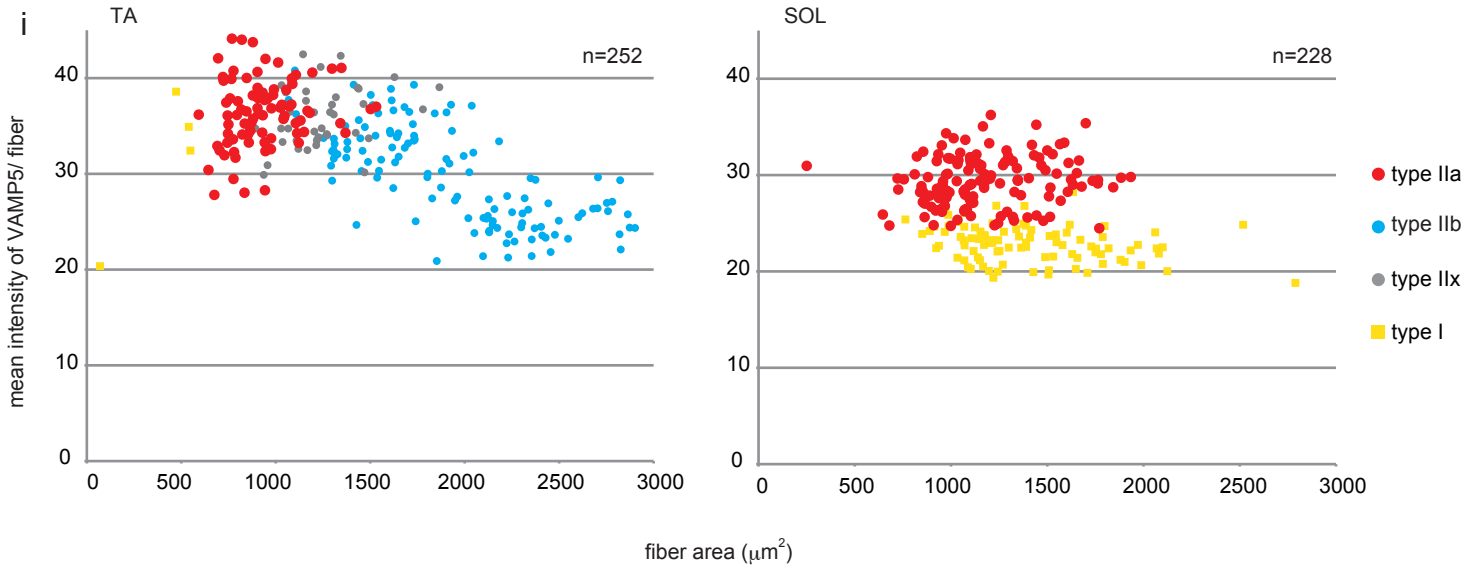
i
TA
n=252
SOL
n=228
mean intensity of VAMP5/ fiber
fiber area (μm²)
0
10
20
30
40
500
1000
1500
2000
2500
3000
type IIa
type IIb
type IIx
type I

Fig. 4 The expression of VAMP5 during the regeneration of skeletal muscle. Muscle regeneration was induced by cardiotoxin injection into TA muscles. Two serial sections were labeled for VAMP5 and type IIa MyHC or embryonic MyHC at 1 week (a, b) and 3 weeks (c, d) after the cardiotoxin injection. The VAMP5 signals are shown in a_1 and c_1. Type IIa (green in a_2, c_2) and embryonic MyHC (emb, green in b, d) were used as markers of the regeneration process. Actin filaments were labeled with phalloidin (red), and nuclei were labeled with DAPI (blue). Bars = 10 μm.

Figure4

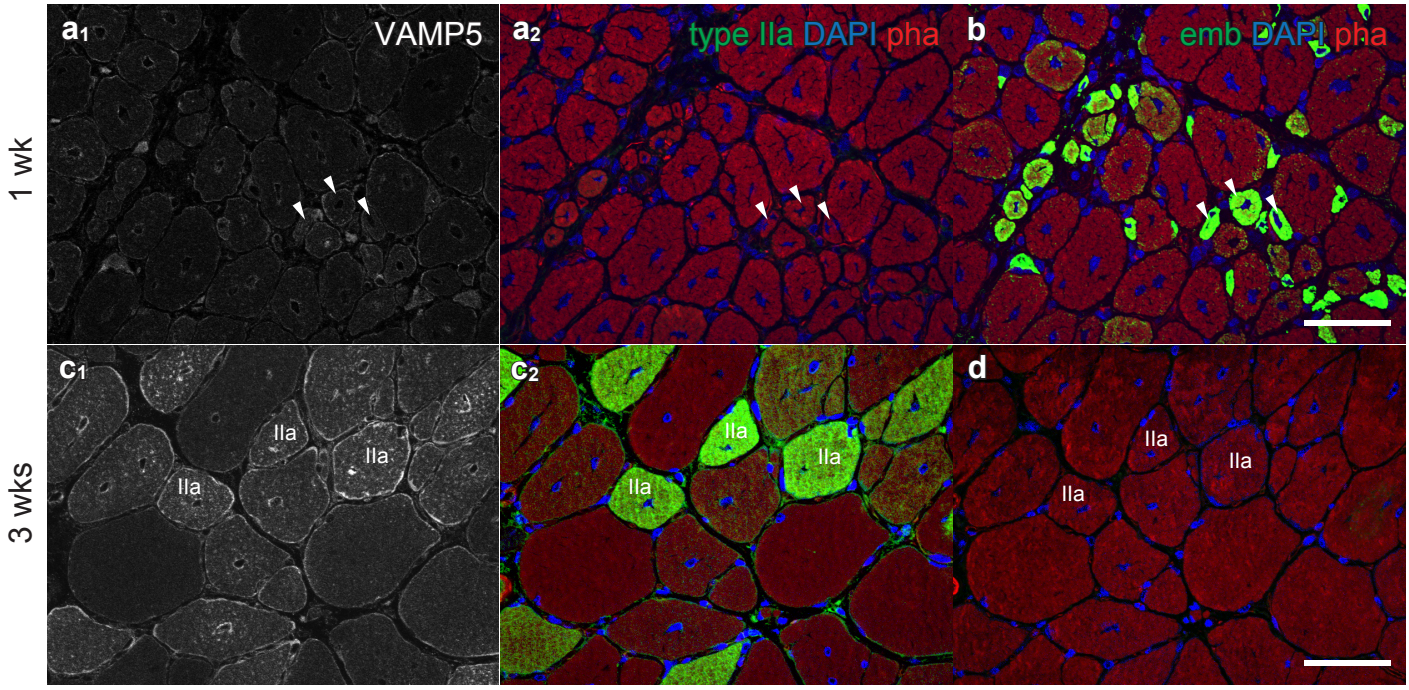
1 wk
3 wks
a1
VAMP5
a2
type IIa DAPI pha
b
emb DAPI pha
c1
IIa
IIa
IIa
c2
IIa
IIa
IIa
d
IIa
IIa
IIa

Fig. 5 A comparison of the VAMP5 and GLUT4 localizations. Transverse sections of TA muscle were double-immunostained for VAMP5 (a_1, b_1) and GLUT4 (a_2, b_2). The merged images are shown in a_3 and b_3. Nuclei labeled with DAPI are indicated in blue. The boxed areas in the top panels were observed at higher magnification levels, and the magnified images are displayed in the bottom panels. The arrows indicate regions that feature the colocalization of VAMP5 and GLUT4. The arrowheads indicate the cytoplasmic regions that were positive for only VAMP5 (filled) or only GLUT4 (open). Bar = 10 μm.

Figure5

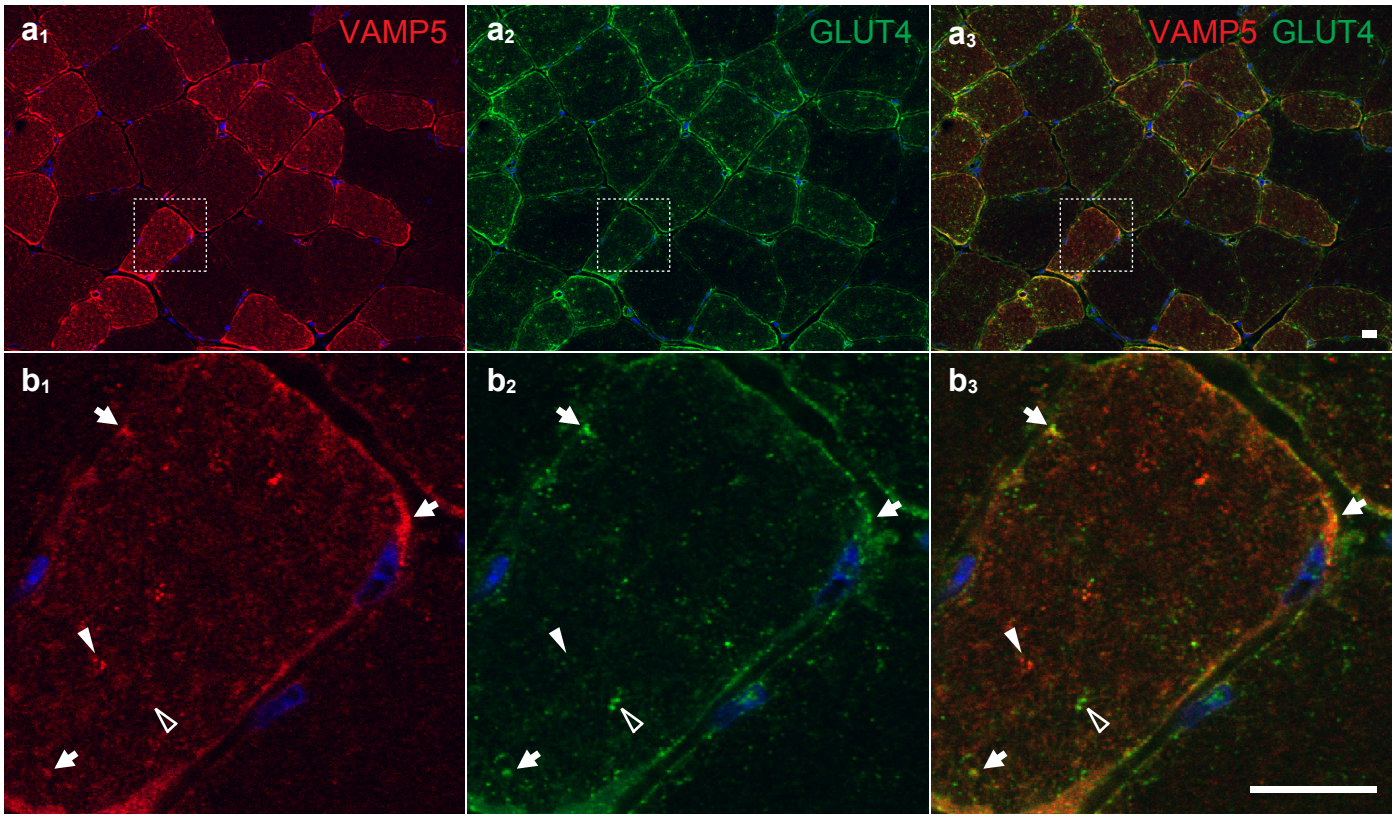

Fig. 6 The localization of VAMP5 in cardiac muscle. Sections of the cardiac muscle were immunostained for VAMP5 (a_1, b_1, c_1 and d_1), and cardiomyocytes are shown longitudinally (a and b) and transversely (c and d). Actin filaments and nuclei are shown in green and blue (a_3, b_3, c_3 and d_3), respectively. VAMP5 was detected strongly around the end of the cardiomyocytes (closed arrowheads), and the perinuclear regions (open arrowheads). The weak signals were also seen in the cytoplasm (arrows in c). These signals of VAMP5 were abolished by the addition of excess recombinant VAMP5 protein (b and d). Sections were double-immunostained for VAMP5 (e_1, f_1 and g_1) and three different markers for intercalated disc junctions; adherence junctions (N-cadherin, e_2), desmosome (desmoplakin, f_2) and gap junction (connexin 43, g_2). The merged images with VAMP5 (red), intercalated disc (green), and nuclei (blue) are shown (e_3, f_3 and g_3). Bars = 10 μm.

Figure6

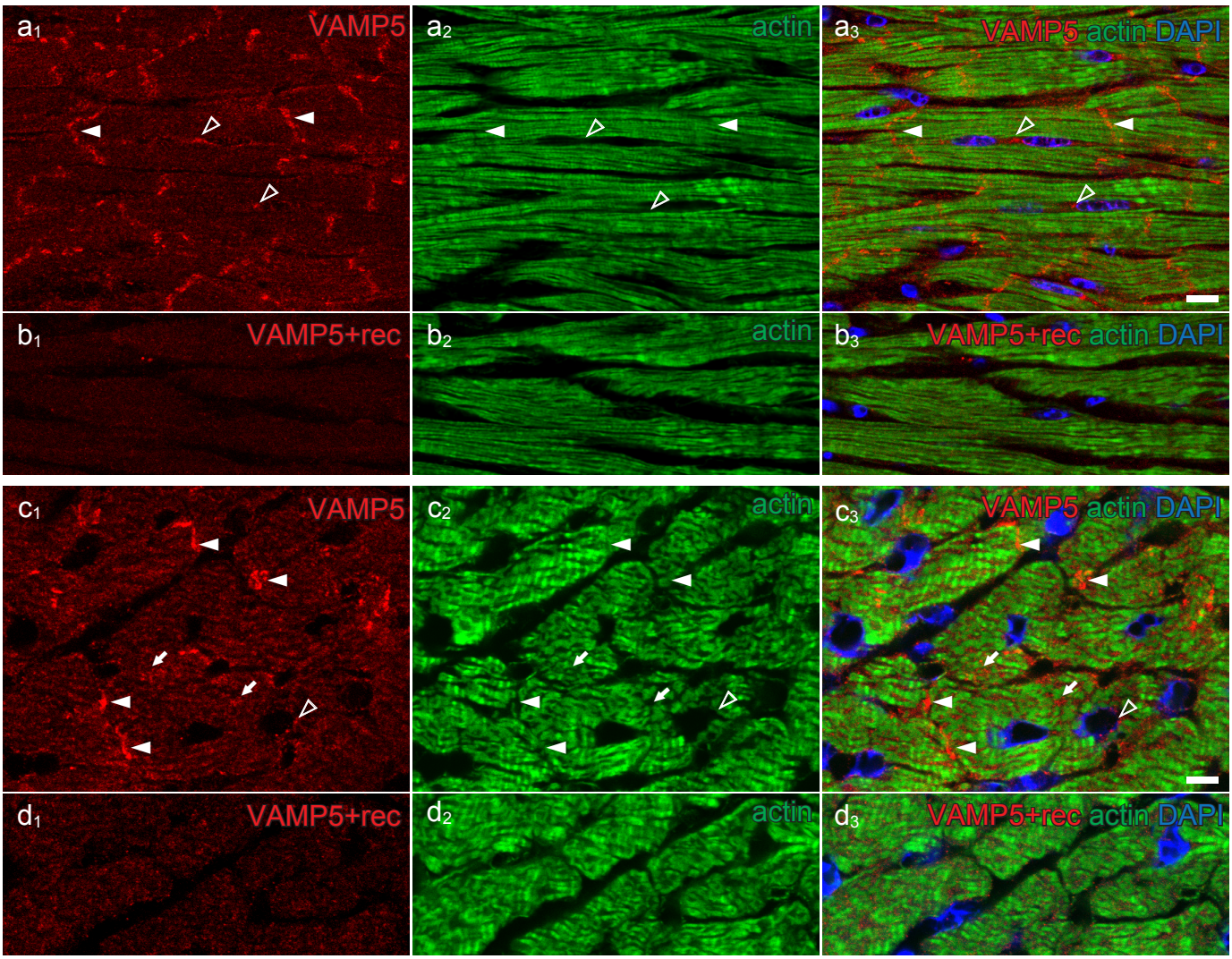
a1 VAMP5
a2 actin
a3 VAMP5 actin DAPI
b1 VAMP5+rec
b2 actin
b3 VAMP5+rec actin DAPI
c1 VAMP5
c2 actin
c3 VAMP5 actin DAPI
d1 VAMP5+rec
d2 actin
d3 VAMP5+rec actin DAPI

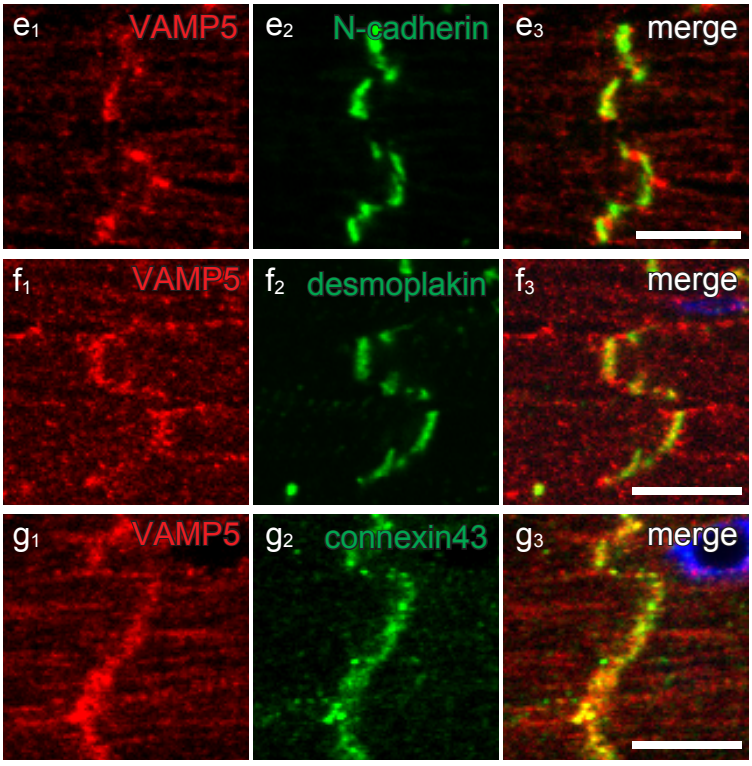
e1 VAMP5
e2 N-cadherin
e3 merge
f1 VAMP5
f2 desmoplakin
f3 merge
g1 VAMP5
g2 connexin43
g3 merge